Solvent-Induced Conformational Changes of *O*-Phenyl-cinchonidine: A Theoretical and VCD Spectroscopy Study

Angelo Vargas, Norberto Bonalumi, Davide Ferri, and Alfons Baiker*

Department of Chemistry and Applied Biosciences, Swiss Federal Institute of Technology, ETH Hönggerberg, CH-8093 Zurich, Switzerland

Received: September 5, 2005; In Final Form: November 23, 2005

The conformational analysis of the synthetic chiral modifier *O*-phenyl-cinchonidine (PhOCD) used in enantioselective hydrogenations over noble metal catalysts has been performed at a PM3 semiempirical level in vacuum. The minimum energy conformations calculated at the DFT level with a medium-size basis set have been compared to those of the parent alkaloid cinchonidine (CD). PhOCD behaves similarly to CD and shows four main conformers, denoted as Closed(1), Closed(2), Open(3), and Open(4). Open(3) is found to be the most stable in vacuum and in CH_2Cl_2 and CCl_4 solvents. A comprehensive normal-mode analysis has been performed for these conformers, and assignment of the infrared spectrum of PhOCD in CCl_4 ($\epsilon = 2.2$) has been performed using the calculated spectrum of Open(3), which appears to be the most populated in this solvent. A combined theoretical−experimental VCD spectroscopy approach was used to increase the spectroscopic sensitivity toward changes in the distribution of conformers upon change of solvent polarity. The VCD spectra confirm that Open(3) is by far the most stable conformation in CCl_4 ($\epsilon = 2.2$) and indicate that an excess Closed(2) conformer has to be expected in CD_2Cl_2 ($\epsilon = 8.9$). The possible influence of this conformational behavior is discussed on the basis of available catalytic data and in relation to the enantioselective potential of PhOCD as a chiral modifier on supported metal catalysts.

1. Introduction

Besides their extensive use as chiral catalysts and ligands in asymmetric synthesis,[1] cinchona alkaloids are by far the most widely used chiral surface-modifiers in the enantioselective hydrogenation of C═O and C═C bonds on supported noble metal catalysts. The catalytic system consisting of chirally modified platinum was first discovered by Orito for the asymmetric hydrogenation of α-ketoesters[2] and was extended successively to a variety of other substrates, making it the most versatile among enantioselective heterogeneous catalysts. Excellent recent reviews cover the scope of substrates, modifiers, and several other aspects related to the efficiency of the catalytic chiral metal surface.[3−5] The underlying principle for the efficiency of this catalytic system is the modification of the metal surface of a supported metal catalyst (e.g., Pt, Pd, Rh) by means of a chiral molecule (the cinchona alkaloid) and the consequent generation of chiral sites capable of discriminating between the pro-chiral faces of C═O and C═C bonds.

It is well-known that cinchona alkaloids that are in near-enantiomeric relationships are able to afford opposite enantiomers,[6] but it has also been discovered recently that cinchona ether homologues can afford opposite enantiomers though maintaining the same absolute configuration of the parent alkaloid.[7] Hence, surface chiral sites can be fine-tuned effectively by functionalization of the original modifier. A nice feature of this system is that the different adsorption energies of differently substituted cinchona alkaloids allow for competition at surface sites that can trigger the switch of the enantioselective properties of a modified metal.[8,9] The synthetic alkaloid *O*-phenyl-cinchonidine (PhOCD) is one of the most interesting modifiers able to trigger the switch of the enantioselective properties of a metal, and several studies underline its potential as novel surface modifier.[7,8,10−13]

There is strong evidence that the conformation of a cinchona alkaloid can be critical for the extent of the final enantioselectivity. For example, the change of solvent polarity greatly affects the enantioselectivity of asymmetric reactions that are catalyzed by cinchona alkaloids.[14,15] Moreover, in the enantioselective hydrogenation of ketopantolactone on cinchonidine-modified platinum, the achieved enantiomeric excess exhibits about the same solvent dependence as the fraction of conformer Open(3) in solution.[16] The importance of the dependence of the conformation of the cinchona modifier on the nature of the solvent is best illustrated by the behavior of the synthetic modifier pantoyl-naphthylethylamine (PNEA) in the same reaction, which retains the essential submolecular entities required to induce enantioselectivity (anchoring group, aliphatic N atom and chiral center).[17] The enantiomeric excess depends on the conformational rigidity of the modifier that is attained only in acidic media.

To our knowledge, the only cinchona ether whose conformational space has been studied as function of solvent polarity is methoxydihydrocinchonidine.[18] More complex ethers used in asymmetric dihydroxylation have been investigated, however, without focusing on solvent effects on conformational behavior.[19] Given the interesting reactivity of PhOCD and the importance of mechanistic studies for the engineering of chiral surfaces, we addressed our investigations to some basic aspects of this interesting molecule. A frequent approach to understanding the catalytic action of cinchona alkaloids consists of studying their conformational space in vacuum and in the presence of solvents in order to identify those conformations that are more likely to take part actively in the catalytic process.[16,18,20]

* Corresponding author. E-mail: baiker@chem.ethz.ch. Phone: +41 044 632 31 53. Fax: +41 044 632 11 63.

10.1021/jp055013j CCC: $33.50
Published on Web 12/27/2005

TABLE 1: Electronic Energy Differences and Gibbs Free Energy Differences (kcal/mol), Dipole Moments (μ, Debye), and Angles τ_1 and τ_2 for the Optimized Conformations of Cinchonidine and *O*-Phenyl-cinchonidine[a]

conf.	Open(3)	Closed(1)	Closed(2)	Open(4)	Open(5)	Open(5)′	Open(6)
				CD			
ΔE_{el}	0.0	1.7	2.4	2.7	5.7	1.0	5.0
ΔG	0.0	2.9	3.9	4.3	7.3	3.6	7.0
μ	1.7	2.3	2.7	1.8	2.1	3.8	1.6
τ_1	282	73	264	91	263	277	84
τ_2	152	58	69	151	314	275	306
				PhOCD			
ΔE_{el}	0.0	1.7	1.9	2.9	5.3		6.8
ΔG	0.0	2.4	2.2	3.7	6.6		7.4
μ	1.8	2.7	2.9	1.9	2.5		2.2
τ_1	282	58	259	90	265		82
τ_2	153	74	63	152	309		306

[a] Open(5)′ is the Open(5) conformation with an internal hydrogen bond. The level of theory is DFT/B3LYP using the 6-31Gdp basis set.

The conformation of PhOCD in solution is analyzed using a theoretical−experimental approach consisting of calculating the theoretical infrared and VCD spectra of its most stable conformers and using them as templates to identify the conformer distribution in the experimental spectra measured in solvents with different polarities. This method already showed a great potential in revealing the relative population of the conformers of cinchonidine and (*R*)-2-(pyrrolidin-1-yl)-1-(1-naphthyl)ethanol in $CDCl_3$.[21] Here, this potential is demonstrated using different solvents. Finally, a comprehensive normal-mode analysis of PhOCD is also presented, which should provide a possible basis for future studies devoted to the understanding of the role and behavior of PhOCD as a chiral auxiliary in enantioselective catalysis.

2. Experimental Section

2.1. Theoretical Calculations. All theoretical calculations were performed using the Gaussian 98[22] and Gaussian 03[23] sets of programs. The potential energy surfaces (PES) were determined using a PM3 Hamiltonian[24] on a grid of 1296 (36 × 36) calculated points. The structures of the molecules were initially optimized using the PM3 semiempirical Hamiltonian; then the obtained geometries were used as starting points for the generation of the 36 × 36 grid by stepwise rotation around the C(4)′−C(9) and C(9)−C(8) bonds and full PM3 optimization of the molecule, except for the fixed τ_1 and τ_2 angles. The minimum-energy conformations were reoptimized using density functional theory (DFT) with the Becke's three parameter hybrid method[25] and using the Lee−Yang−Parr correlation functional.[26] A 6-31Gdp basis set of Pople and co-workers[27] was used for all calculations. ΔG was calculated using the standard statistical mechanics expressions for an ideal gas in the canonical ensemble. For this, gas-phase vibrational energies were calculated at the same level of theory used for the geometry optimization. The values for the τ_1 and τ_2 angles of the minimum energy conformations of CD and PhOCD calculated at the PM3 level of theory (available as Supporting Information) show a good qualitative agreement with the more refined DFT calculations shown in Table 1. Solvent effects were accounted for with a self-consistent reaction-field calculation using a cavity determined self-consistently from an isodensity surface (SCIPCM),[28] as implemented in Gaussian 03.[23] Single point calculations were performed on the optimized geometry obtained from the calculated minima in vacuum. Five thousand and four hundred integration points were used with a single center integration procedure. A value of 0.0004 au was chosen as the isodensity level. Molden was used as the graphical interface.[29]

2.2. FT-IR Spectroscopy. The Fourier transform infrared spectra of PhOCD solutions (0.01 mol l^{-1}) were collected in the transmission mode at 4 cm^{-1} resolution using a Bruker Optics Tensor27 spectrometer equipped with a liquid cell (CaF_2 windows, 1 mm path length) and a DTGS detector.

2.3. Vibrational Circular Dichroism Spectroscopy. The VCD spectra of PhOCD solutions were measured using a PMA37 accessory (Bruker Optics) equipped with a liquid-nitrogen-cooled MCT detector, a photoelastic modulator, a polarizer, a lock-in amplifier, and a low-pass filter (<1800 cm^{-1}). Infrared radiation is provided through a Vector33 infrared spectrometer (Bruker Optics). Prior to measurement of solute samples, a VCD spectrum of a CdS sample wavelength plate combined with a second polarizer was measured to determine the phase followed by measurement of a single channel spectrum of neat solvent serving as a reference for calculating absorbance spectra. A VCD spectrum of the neat solvent was subtracted from the VCD spectrum of the solute. The instrument and the procedure have been described in detail elsewhere.[21] Spectra were collected with a CaF_2 cell equipped with a 1-mm-path-length Teflon spacer by coadding 3500 scans at 4 cm^{-1} resolution.

2.4. Enantioselective Hydrogenations. Catalytic enantioselective hydrogenations of ketopantolactone were performed in a parallel pressure reactor system Endeavor (Argonaut Technologies), with eight mechanically stirred stainless steel reactors equipped with glass liners. A standard procedure has been followed for the prereduction of the catalyst (Pt/Al_2O_3, Engelhard E4759) and for catalytic hydrogenation.[30]

2.5. Materials. *O*-Phenyl-cinchonidine (Ubichem), cinchonidine (Fluka, 98%), ketopantolactone (Hoffmann-La Roche), and CCl_4 (Merck, 99.8%), $CDCl_3$ (Merck, 99.8%), CD_2Cl_2 (Sigma-Aldrich, 99.5%), cyclohexane (Aldrich), and CS_2 (Fluka, puriss.) solvents were used without further purification.

3. Results

3.1. Conformational Analysis of O-Phenyl-cinchonidine versus Cinchonidine. Cinchona alkaloids are composed of two rigid moieties, namely, a quinoline and a quinuclidine ring, connected by a Csp_3 hydroxilated carbon atom (C(9)). Hindered rotation is possible around the two bonds connecting the two moieties. The conformation of several cinchona alkaloids has been investigated in few studies,[16,18−20,31−33] the general result being that only rotation around the C(4)′−C(9) and C(9)−C(8) bonds is important to a first approximation for the major conformational changes of these molecules. The angles associated with these rotations are shown in Figure 1 together with a definition of the direction of rotation used to determine the potential energy surfaces (PES) of Figure 2. These are defined on the subspace identified by angles τ_1 and τ_2 of the molecule.

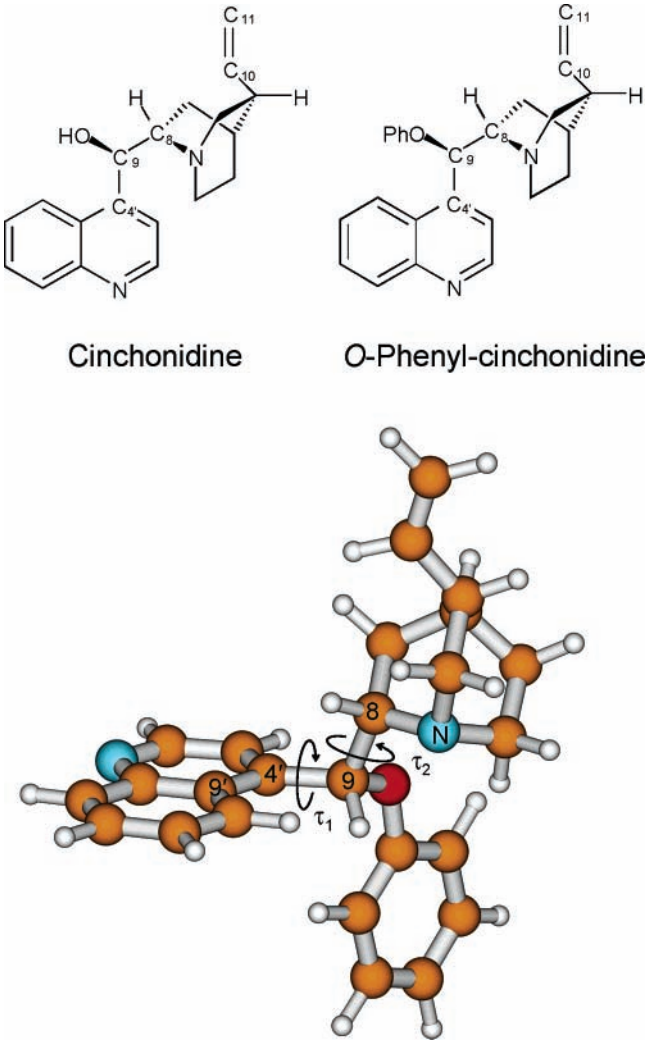

Figure 1. Molecular structure of cinchonidine (CD) and *O*-phenyl-cinchonidine (PhOCD). Angles of rotation τ_1 and τ_2 are defined by the dihedral angles 9′−4′−9−8 and 4′−9−8−N, respectively. The directions of rotation used to generate the PES are shown in the figure.

The conformational behavior shown by the semiempirical PES for cinchonidine (CD) and *O*-phenyl-cinchonidine (PhOCD) is essentially the same, showing that the mostly populated angles are in the same region of the subspace. The search was refined by DFT calculations on the six most stable conformers, which lead to the structures depicted in Figure 3. Structural and energetic data are reported in Table 1 for the two alkaloids at the same level of theory and are rather closely related. Values of differences between the dipole moments of open and closed conformers are slightly larger for the ether derivative, which should correspond to a larger conformational sensitivity to the polarity of the solvent. Open(5)′ is a conformation of CD that exhibits an internal hydrogen bond (Figure 4). It is interesting to note that unlike what was reported in previous studies, the Open(5)′ conformation of CD is energetically quite close to the Closed(2) conformation in terms of Gibbs free energy (Table 1). In principle, an Open(6)′ conformation could also exist for CD but a minimum energy structure was not found at this level of theory. Attempts to compute an Open(6′) conformation reveals that its energy tends to be around 2 kcal/mol higher than the Open(5)′, indicating that the internal hydrogen bond plays little role for the Open(6). Such structures with intramolecular bonding cannot be formed in the case of PhOCD, which is one of the obvious differences between the parent alkaloid CD and its ether derivatives in vacuum.

Interestingly, it results from the ΔG values in Table 1 that the conformation of PhOCD in vacuum that is closer in energy to the Open(3) is the Closed(2), whereas it is the Closed(1) in the case of CD. This is consistent with what was reported for the only other cinchona ether whose conformations have been analyzed, namely, methoxydihydroquinidine, which is present as a mixture of Open(3) and Closed(2) conformers in several solvents.[18]

Table 2 gives the calculated energies of stabilization of the conformers with respect to the energies calculated in vacuum, for the solvents CH_2Cl_2 and CCl_4. The stabilization due to the solvent effect increases with the dielectric constant and is proportional to the dipole moment. CH_2Cl_2 has a more pronounced stabilization effect on the closed conformers, having a larger dipole moment, than on the open conformers. This differential stabilization also exists for CCl_4 but is less pronounced. The results above indicate that solvents with higher dielectric constants should increase the population of the closed conformers more than solvents having lower dielectric constants,[34] in line with what was observed already for the parent alkaloid CD.[16]

3.2. Infrared Spectra of *O*-Phenyl-cinchonidine Solutions and Assignment of Normal Modes. PhOCD belongs to the C_1 point group and has 156 fundamental vibrations, which are both infrared and Raman active. Being a related derivative of

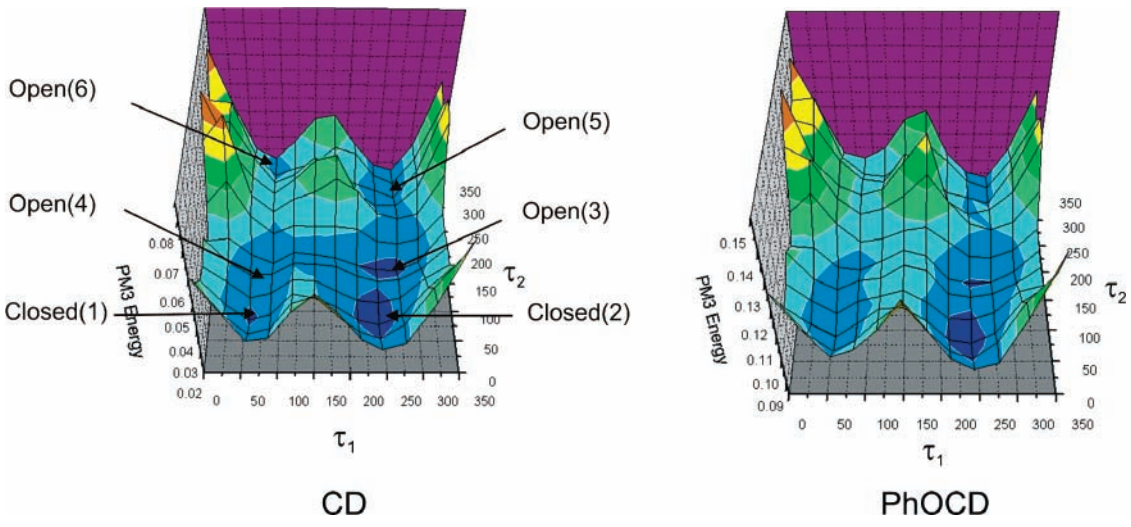

Figure 2. Potential energy surfaces of cinchonidine (CD) and *O*-phenyl-cinchonidine (PhOCD).

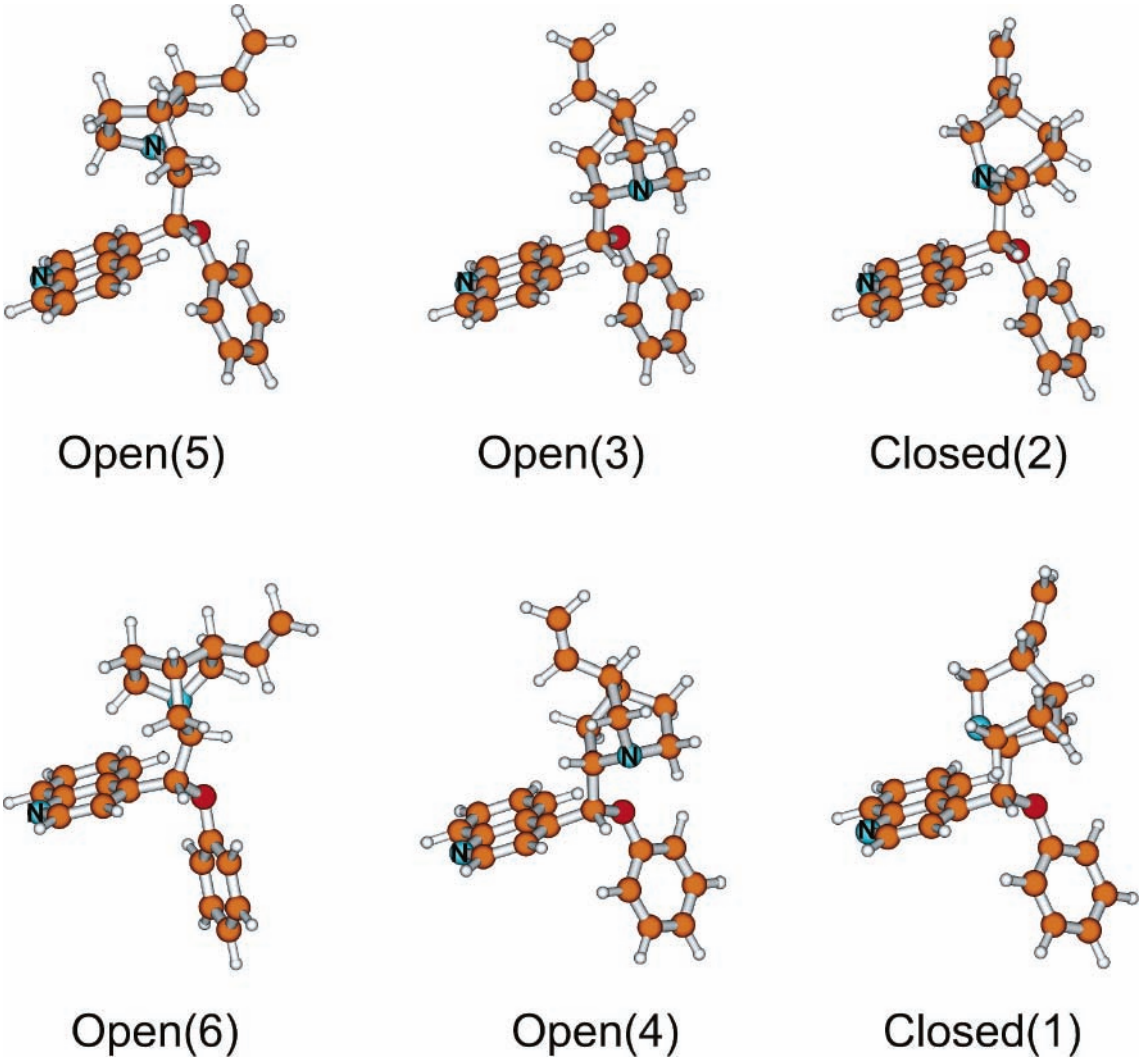

Figure 3. Minimum energy conformations of *O*-phenyl-cinchonidine in vacuum.

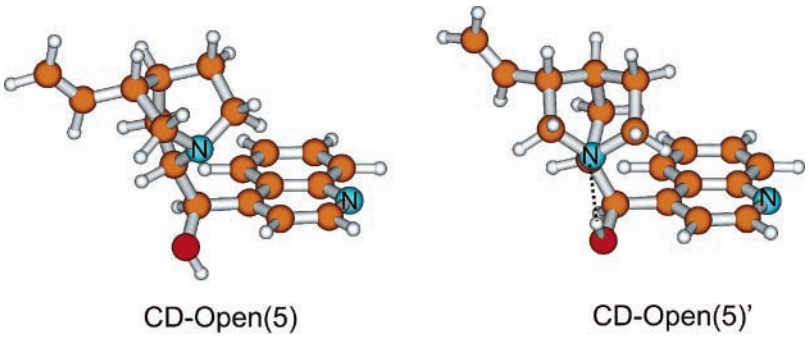

Figure 4. Open(5) and Open(5)′ conformations of cinchonidine.

TABLE 2: Calculated Stabilization Energies (in kcal/mol) of the *O*-Phenyl-cinchonidine Conformers due to the Effect of Solvents CH_2Cl_2 and CCl_4[a]

	Open(3)	Closed(1)	Closed(2)	Open(4)
CH_2Cl_2	3.7	4.4	4.4	4.0
CCl_4	1.8	2.1	2.1	1.9

[a] The values are obtained on single point energies at the gas-phase minima.

CD, assignment of most of these vibrational modes can be achieved by comparison with CD,[35,36] quinoline[37,38] and quinuclidine.[39] Assignment of signals in the 1650−1450 cm^{-1} spectral region has been reported already for adsorption purposes.[9] Besides the primary literature, characteristic frequency tables were also used for the assignment[40,41] and calculated modes were visualized using the GaussView interface.[22] Moreover, PhOCD exhibits a rich conformational chemistry similar to CD, which is, in principle, strongly dependent on the solvent; that is, the population of the cinchona conformers changes with increasing solvent polarity.[16,18,20,42] This fact makes analysis of the conformation of PhOCD in solvents a needed step for understanding the functioning of PhOCD as a possible chiral catalyst or modifier.

The choice of the solvents is based on the relative simplicity of CCl_4, $CDCl_3$, CD_2Cl_2, cyclohexane, and CS_2 spectra with respect to other organic solvents such as toluene and alcohols, whereas the use of deuterated solvents instead of common

TABLE 3: Assignment of the Normal Modes of *O*-Phenyl-cinchonidine in CCl_4 and CD_2Cl_2 Solutions[a] and of Its Conformers Open(3) and Closed(2)

	obs. fundamentals		B3LYP 6-31G(d,p)[e]		
no.	CCl_4	CD_2Cl_2	Open(3)	Closed(2)	assignment
			all signals in the 1650−1100 cm^{-1} spectral region		
130	1637	1635	1670	1670	νC═C, V[b]
129	1614	1614	1620	1620	ring def., Q[b]
128	1598	1599	1609	1609	ring def., Ph[c]
127	1589	1589	1595	1593	ring def., Q + ring def., Ph
126			1591	1590	ring def., Q + ring def., Ph
125	1570	1570	1570	1571	ring def., Q
124	1508	1508	1509	1511	ring def., Q
123	1494	1495	1491	1491	ring def. + bC−H, Ph
122			1477	1478	$\delta_s(CH_2)$, QD
121	1465	1466	1464	1463	$\delta_s(CH_2)$, QD
120	1454	1454	1458	1459	$\delta_s(CH_2)$, QD (Open) + ring def., Q
119			1457	1458	$\delta_s(CH_2)$, QD + ring def., Q (Open)
118			1453	1454	ring def. + bC−H, Ph (Open); $\delta_s(CH_2)$, QD (Closed)
117			1451	1453	$\delta_s(CH_2)$, QD (Open); ring def. + bC−H, Ph (Closed)
116			1424	1424	bC−H, V
115	1423	1423	1422	1422	ring def., Q
114	1392	1392	1388	1386	C(9)−H and C(8)−H def. (Open) + ring def., Q
113	1383	1385	1380		C(8)−H def. + ring def., Q (Open)
113				1371	C(9)−H and C(8)−H def.
112	1360	1360	1366		C(9)−H and C(8)−H def.
112				1357	C(9)−H + ring def., Q
111			1350		ωC(9)−H and ωC−H, QD
111	1346	1346		1341	ωC(9)−H and ωC−H, QD
110			1345		ωCH_2, QD
110				1341	ωC(9)−H + ωC(8)−H and ωC−H, QD
109	1337	1339	1340	1336	ωCH_2, QD
108			1332	1334	ωCH_2, QD + ωC(9)−H (Closed)
107	1323	1323	1325	1326	ring def., Ph
106			1320		ωCH_2, QD
105			1318	1318	ωCH_2, QD
105				1314	ωCH_2 and tCH_2, QD
104			1308	1309	ωCH_2, QD + bCH, Q
103	1301	1303	1304	1304	ωCH_2, QD + bCH, Ph
102			1299	1299	rC−H, vinyl + bCH (Closed)
101				1298	rC−H, vinyl + bCH, Ph
101			1296		ωCH_2, QD (Open)
100			1293	1292	ωCH_2, QD
99	1288	1290	1283	1282	rC−H, V
98			1270	1272	ωC(9)−H + tCH_2, QD; ring def., Q (Closed)
97	1261	1261	1256	1255	ωC(9)−H + tCH_2, QD
96			1247		tC(9)−H + tCH_2, QD + bCH, Q
96				1238	tCH_2, QD + bCH, Q
95			1236	1235	tC(9)−H (Open) + tCH_2, QD + νO−C_{Ph} + bCH, Q
94	1236	1238	1231		νO−C_{Ph} + tCH_2, QD
93			1229	1229	bCH, Q
93				1226	tCH_2, QD + bCH, Q
92			1217	1218	tCH_2, QD
91	1211	1213	1206		bCH, Q
91				1210	bCH, Q
90			1196	1191	tCH_2, QD
89	1173	1174	1166	1167	bCH, Ph
88	1163	1163	1163	1162	tCH_2, QD + bCH, Q (Open)
			major signals in the 1100−860 cm^{-1} spectral region		
82	1088	1087	1080	1079	bCH, Ph + νC(9)−C(8) (Closed)
81			1072		bCH, Ph + bCH, Q + νC(9)−C(8)
80	1072	1073	1069		νCC and bCH, Q + bCH, Ph
79			1060		tCH_2 and νCC, QD
78				1042	νCC and tCH_2, QD
77	1043	1043	1032	1034	νC−N−C and tCH_2, QD + rCH, vinyl (Open)
76				1029	rCH_2 and νC−N−C, QD
76	1029	1029	1025		νCC, QD + bCH, Ph

TABLE 3 (Continued)

	obs. fundamentals		B3LYP 6-31G(d,p)[e]		
no.	CCl_4	CD_2Cl_2	Open(3)	Closed(2)	assignment
			major signals in the 1100−860 cm^{-1} spectral region (cont'd)		
72			1003		ωCH, V
71	991			991	rCH, V + rCH_2, QD
70				984	bCH, Q
69			978		ring stretch, Ph and Q
67				967	tCH_2, QD
62	939		933		rCH_2, QD + rCH, V
61			919		νCC, QD
60	914		910	911	ωCH, V
59			908		ωCH, V + rCH_2, QD
57	879		869		ωCH, Ph and Q
			other major signals in the 860−700 cm^{-1} spectral region[d]		
56				854	ωCH, Q
55				850	ωCH, Q
53			821		rCH_2, QD + ωCH, Q + ring stretch, Ph
52				817	ωCH, Q + rCH_2, QD
48			818		rCH_2 and νCC, QD
48				781	ring stretch, Ph + νCC, QD
45			753	753	ωCH, Q
44				749	ωCH, Q
43			743	743	ωCH, Ph

[a] Concentration: 10 mM. [b] Consistent with assignment in refs 35 and 36 and refs therein. [c] Consistent with assignment in ref 9. [d] Not observable in CCl_4 and CD_2Cl_2. [e] Scaled by 0.97. Q = quinoline, QD = quinuclidine, Ph = phenyl, V = vinyl, def. = deformation, stretch and ν = stretching, b = bending, ω = wagging, t = torsion, r = rocking.

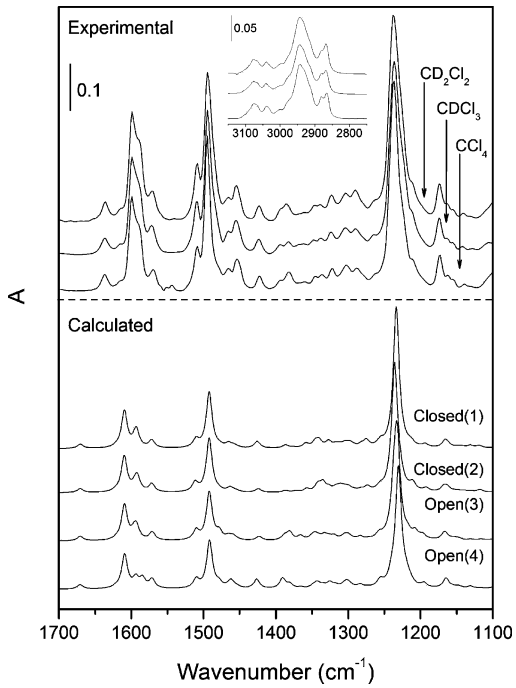

Figure 5. Experimental transmission infrared spectra (top) of *O*-phenyl-cinchonidine in CCl_4, $CDCl_3$, and CD_2Cl_2 at ambient temperature and calculated vibrational spectra (bottom) of the most stable conformers between 1700 and 1100 cm^{-1}. The inset shows the 3150−2750 cm^{-1} spectral region of the experimental spectra. Frequencies of calculated spectra were scaled by 0.97. Conditions: $C_{PhOCD} = 0.01$ mol l^{-1}.

hydrogenated analogues offers the possibility of sampling spectral regions otherwise strongly shadowed.

The transmission infrared spectra of PhOCD solutions in CCl_4, $CDCl_3$, and CD_2Cl_2 shown in Figure 5 in the 1700−1050 cm^{-1} spectral region are dominated by the typical vibrational modes of the phenyl and quinoline rings (above 1450 cm^{-1}) and by the stretching mode of the ether connectivity (O−C_{Ph}, ca. 1240 cm^{-1}). The spectra strongly resemble each other, and minor differences are found in the broadening of the signals at 1494 and 1240 cm^{-1} and in the 1400−1200 cm^{-1} spectral region. In the high-frequency region (inset), envelopes are observed at 3076, 3039, 3001, 2943, 2881, and 2866 cm^{-1}, which are assigned to the stretching vibrations of the vinyl group and of the phenyl, quinoline, and quinuclidine (below 2980 cm^{-1}) rings and will not be discussed in detail in the present work.

Figure 5 also displays the calculated vibrational spectra of the most stable conformers observed in vacuum, that is, Open(3), Closed(2), Open(4), and Closed(1) whose frequencies have been scaled by 0.97. The description of the fundamental modes is given in Table 3 only for Open(3) and Closed(2) according to the discussion that follows. Moreover, differences are observed in the description of some normal modes of Open(3) and Closed(2), some of which are discussed below because of their possible relevance for understanding solvent induced conformational changes. Table 3 also presents the assignment of fundamental vibrations below the cutoff of the CCl_4 and CD_2Cl_2 solvents that show high intensity (>10 in the calculated spectra) and may be of use for further spectroscopic studies on PhOCD on metal surfaces using techniques where this region is accessible.

The calculated spectra, in general, reproduce the experimental spectra in the different solvents well. Some incongruity is found for the vibration corresponding to the stretching mode of the vinyl group (1722 cm^{-1}, $\Delta\nu = \nu_{caldc} - \nu_{exptl} = 33$ cm^{-1}) and for the quadrant stretch of the phenyl ring at 1599 cm^{-1} ($\Delta\nu =$ 11 cm^{-1}). However, the assignment is accomplished easily on the basis of primary literature.

At a first glance, comparison of the spectrum in CCl_4 with the calculated spectra of the four conformers suggests that the Open conformers contribute to a larger extent to the experimental spectrum. These species present a low-energy shoulder of the signal at 1494 cm^{-1} and some signals between 1410 and 1360 cm^{-1}, which are absent in the calculated spectra of the Closed conformers. The shoulder is calculated at ca. 1477 cm^{-1}

and belongs to scissor modes of the methylene groups of the quinuclidine moiety, which in the Open conformers possess a dipole moment perpendicular to that of the Closed conformers and is normal to the plane of the quinoline ring. Moreover, it appears reasonable to also exclude the presence of the conformer Open(4). The most striking deviation of the spectrum of Open-(4) is the presence of a clear doublet at 1592 and 1584 cm^{-1}, whose shift (8 cm^{-1}) is larger than for the other conformers (2−4 cm^{-1}). The two signals are associated with a quadrant stretch of the phenyl ring and with a ring deformation mode of the pyridine ring of quinoline (ν(C═C) and ν(C═N)), respectively. The former mode degenerates in the case of Open(3) and the Closed conformers, and additionally couples with the latter mode. However, the calculations indicate that the contribution of the mode involving the quinoline ring prevails in the vibration at high frequency (1595 cm^{-1}) only in Open(3), whereas in Closed(1) and Closed(2) the high-frequency vibrations (1593 and 1592 cm^{-1}, respectively) are dominated by the mode of the phenyl ring. The small $\Delta\nu$ in Open(3), Closed(1), and Closed(2) more likely generates the single band at 1589 cm^{-1} in the experimental spectrum.

The absence of Open(4) from the spectra of PhOCD in CCl_4 is in agreement with the large difference in energy compared to Open(3) (Table 1). Similar results were found for other cinchona alkaloids.[16,18] The values of the dipole moment of the two Open conformers are very similar so that the difference in energy renders the observation of Open(4) in polar solvents improbable. Polar solvents should stabilize the conformers exhibiting higher dipole moment as shown by the calculations. This allows us to omit Open(4) from further consideration in the following because of the higher polarity of our next solvent, CD_2Cl_2. On the basis of the exclusion of Open(4) and the Closed conformers we give a comprehensive assignment of the infrared signals observed in CCl_4 in Table 3 mainly according to the calculated spectrum of Open(3).

Another important difference between the calculated spectra of the conformers is the origin of the signal centered at ca. 1240 cm^{-1}. As mentioned above, the signal is unequivocally assigned to the stretching mode of the ether group (ν(O−C_{Ph})), which changes slightly from conformer to conformer (1231 cm^{-1} for Closed(1) and Open(3), 1235 cm^{-1} for Closed(2)). However, a strong contribution to this band in the Open(3) conformer is also given by the signal calculated at 1236 cm^{-1}, which is a deformation mode of C(9)−H coupled with the twisting of the methylene groups of the quinuclidine moiety. This accounts for the shoulder at higher energy observed for Open(3) (Figure 5).

The small changes observed in Figure 5 when moving from CCl_4 to $CDCl_3$ and to CD_2Cl_2 do not allow a straightforward determination of the distribution of conformers as in CCl_4. Changes between 1410 and 1330 cm^{-1} suggest an increased population of the Closed species, which would be in agreement with the NMR data reported for methoxy and ester derivatives of dihydroquinidine.[18]

The large dominance of Open(3) in CCl_4 contrasts the data reported for the parent alkaloid CD.[16,18] Close to 40% Closed conformers were determined in benzene,[16] which shows a dielectric constant (ϵ = 2.2) identical to that of CCl_4. This amount is, however, reduced to 30% in toluene (ϵ = 2.3). The almost complete absence of Closed conformers in CCl_4 for PhOCD can be better correlated with the empirical solvent parameter (E_N^T),[43] which is listed together with ϵ in Table 4.

3.3. Distribution of Conformers in Solution using VCD Spectroscopy. Vibrational circular dichroism (VCD) spectroscopy is highly sensitive to changes in the molecular conformation of solutes and is used in the following to further investigate the conformational behavior of PhOCD. The use of VCD to identify the conformers of cinchona alkaloids in solution has been reported only for CD and the synthetic modifier (*R*)-2-(pyrrolidin-1-yl)-1-(naphthyl)ethanol,[21] whereas most previous studies have been performed using NMR.

TABLE 4: Dielectric Constant (ϵ)[a] and Empirical Solvent Parameter (E_N^T)[b] of Some Organic Solvents

solvent	ϵ	E_N^T
CCl_4	2.2	0.052
benzene	2.2	0.111
toluene	2.3	0.099
$CDCl_3$	4.8	0.256
CD_2Cl_2	8.9	0.309

[a] From ref 45. [b] From ref 43.

The VCD spectrum of PhOCD in CCl_4 is initially shortly discussed. The experimental spectrum is disturbed by the interference of the solvent in the 1600−1510 cm^{-1} spectral region. The absorbance of the solvent is also important between 1250 and 1200 cm^{-1} (dotted line in Figure 6), but in contrast to the previous region, the experimental pattern is reproducible and also matches the calculated spectra of the different conformers (with minor deviations). The omission of the Open-(4) structure from further discussion is clearly confirmed by the VCD spectra shown in Figure 6. The calculated spectrum of the Open(3) conformer is again in rather good agreement with the experimental spectrum. Significant are, for example, the signals observed at 1495 (negative, positive in Closed(2)), 1465 (negative, positive in Closed (1)), 1368 (shifted in Closed-(1) and (2)), and 1346 cm^{-1} (negative in Closed(2) and of much lower intensity in Closed(1)). The former signal is the semicircle stretch of the phenyl ring strongly coupled with C−H in plane bendings. The dipole moment associated with this mode is approximately parallel to the plane of the phenyl ring, but it

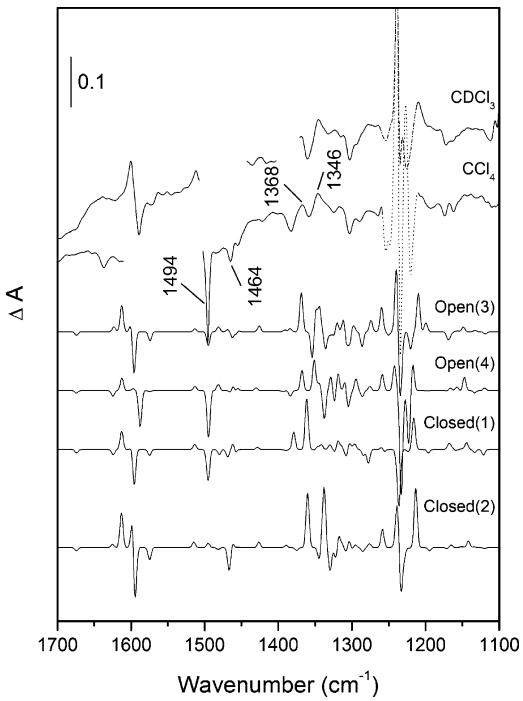

Figure 6. Experimental VCD spectra (top) of *O*-phenyl-cinchonidine in CCl_4 and $CDCl_3$ at ambient temperature and calculated VCD spectra (bottom) of the most stable conformers between 1700 and 1100 cm^{-1}. Areas where strong solvent interference occurs are omitted. Dotted areas represent regions where solvent absorption is important. Conditions: C_{PhOCD} = 0.045 mol l^{-1}.

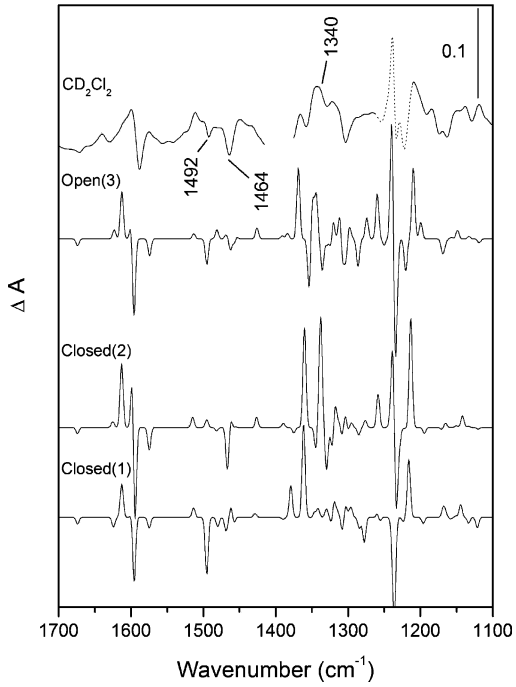

Figure 7. Experimental VCD spectra (top) of *O*-phenyl-cinchonidine in CD_2Cl_2 at ambient temperature and calculated VCD spectra (bottom) of the conformers Open(3), Closed(1), and Closed(2) between 1700 and 1100 cm^{-1}. Areas where strong solvent interference occurs are omitted. Dotted areas represent regions where solvent absorption is important. Conditions: $C_{PhOCD} = 0.045$ mol l^{-1}.

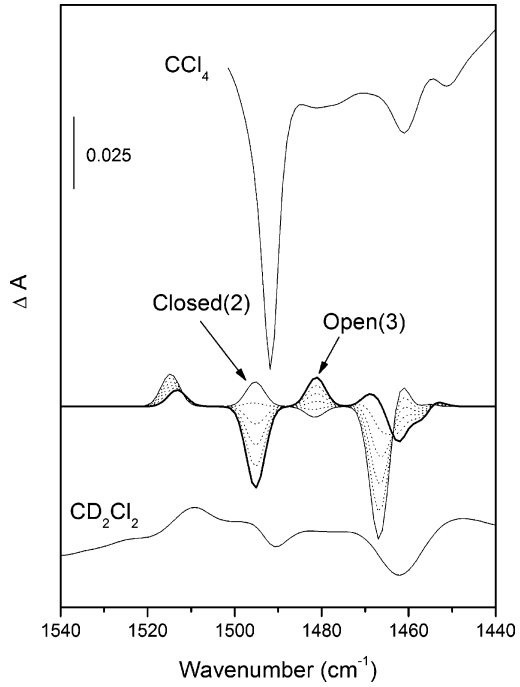

Figure 8. Experimental VCD spectra of *O*-phenyl-cinchonidine in CCl_4 (top) and in CD_2Cl_2 (bottom) and calculated VCD spectra of conformers Open(3) (bold) and Closed(2) in the 1540−1440 cm^{-1} spectral region. Also shown are spectra resulting from the linear combination (dotted) of the calculated spectra of the two conformers in the ratios Open(3)/Closed(2) 80/20, 60/40, 40/60, and 20/80. The spectrum in CCl_4 is affected by solvent absorption above 1500 cm^{-1}. Experimental spectra correspond to the spectra shown in Figure 6 and Figure 7.

exhibits an opposite direction in Closed(2) compared to Open(3) and Closed(1), which accounts for the sign of the signal in the VCD spectrum: positive, negative, and negative, respectively.

The signal at 1368 cm^{-1} can be described as a symmetric deformation of the C(9)−H and C(8)−H bonds for Open(3), which is found above 1370 cm^{-1} with much lower intensity in the Closed conformers.

Particularly good is the matching in the 1250−1200 cm^{-1} spectral region, which is characteristic for the stretching mode of the ether connectivity, as mentioned in the previous section. Hence, the experimental VCD spectrum in CCl_4 confirms the strong predominance of conformer Open(3).

Changing from CCl_4 to $CDCl_3$ does not significantly alter the equilibrium between the conformers (Figure 6) because the VCD spectra resemble each other very much. Solvent interference occurs in this case between 1500 and 1450 cm^{-1} and between 1400 and 1370 cm^{-1}. The 1600−1500 cm^{-1} spectral region is free from interference but does not appear diagnostic because all conformers show similar behavior. As in the case of methoxydihydroquinidine in $CDCl_3$,[18] Open(3) still appears dominant but the changes in the 1250−1200 cm^{-1} spectral region may reveal information on the conformational equilibrium, which is even more evident when moving to CD_2Cl_2.

The VCD spectra of PhOCD were also recorded in cyclohexane ($\epsilon = 2.0$) and CS_2 ($\epsilon = 2.6$) solvents (not shown). In contrast to CCl_4 and $CDCl_3$, assignment of the spectral features to a specific conformer is less straightforward. Nevertheless, the spectrum in cyclohexane presents a region between 1335 and 1280 cm^{-1} where the assignment of the conformation of PhOCD predominantly to Open(3) is feasible.

Figure 7 shows the VCD spectrum of PhOCD in CD_2Cl_2. Solvent interference occurs between 1415 and 1375 cm^{-1}. Inspection of the spectrum and comparison with that of PhOCD in CCl_4 (and $CDCl_3$) clearly shows the growth of a shoulder at ca. 1340 cm^{-1} and a remarkable decrease of the ratio between the bands at 1239 and 1210 cm^{-1}. Only conformer Closed(2) exhibits a positive signal at 1338 cm^{-1} and is the only one to show a pattern similar to that observed in the experimental spectrum between 1250 and 1200 cm^{-1}. The amount of Closed(2) is possibly increased already in $CDCl_3$, as analysis of this region suggests based on this argument (see Figure 6). Conformer Closed(1) exhibits a clearly different spectrum and can be omitted from the following discussion. The Closed(1) conformer is also less stable by 0.2 kcal/mol compared to Closed(2) (Table 1). In contrast, it is more abundant in the case of CD in solvents with high ϵ and is more stable than Closed(2) by 1.0 kcal/mol.

The VCD patterns of conformers Open(3) and Closed(2) deviate from each other in several regions of the spectrum, namely, in the 1540−1440 cm^{-1}, 1400−1290 cm^{-1}, and 1250−1100 cm^{-1} regions. Because the spectrum of PhOCD in CD_2Cl_2 appears as a combination of the two conformers, the relative population was simulated by summing their VCD spectra in different ratios. The spectrum obtained with 40% of Open(3) and 60% of Closed(2) is best matching the experimental spectrum. Figure 8 shows the agreement between simulated and experimental spectra for the 1540−1440 cm^{-1} region and clearly reveals the presence of a large fraction of Closed(2). The VCD spectra of PhOCD in CCl_4 and CD_2Cl_2 are presented in order to better highlight the change in the relative population of the conformers in the two solvents. Note the relatively large difference in solvent polarity and empiric solvent parameter between the two solvents (Table 4). The most important difference between the two conformers in this region is represented by the sign of the VCD signals observed at 1492 cm^{-1} in the experimental VCD spectrum, which was shown to display opposite direction of the dipole moment associated with it. Similar observation holds for the second negative signal at

1464 cm^{-1} in which the molecular dipole moments of the vibrational modes are perpendicular to each other. In contrast to CCl_4, the addition of Closed(2) to Open(3) in large amounts results in the movement of the former band toward the positive sign and of the latter band toward even more negative intensities in CD_2Cl_2, which reproduces the spectrum of Closed(2) well.

The similarity of the spectrum of the Open(3) conformer to that of PhOCD in CCl_4 and of the simulated spectrum to that of PhOCD in CD_2Cl_2 indicates that the fraction of Closed(2) species increases considerably with increasing solvent polarity.

3.4. Implications of Conformational Behavior of *O*-Phenylcinchonidine on its Action as a Chiral Modifier in Enantioselective Heterogeneous Catalysis. The theoretical analysis of the distribution of conformers of PhOCD in vacuum showed that this cinchona alkaloid exhibits similar conformational behavior to that of the parent CD. In solution, the experimental data indicate that the Open(3) and at a lesser extent Closed(2) conformations are the most represented in apolar solvents, with the fraction of Closed(2) increasing significantly with increasing solvent polarity. In particular, in agreement with the behavior reported for methoxydihydroquinidine,[18] the Closed(2) conformation of PhOCD becomes populated in excess relative to the Open(3) when changing from $CDCl_3$ to CD_2Cl_2. In contrast, it has been shown for CD that the ratio Closed(2):Open(3) is 1:3 in this solvent.[16] Therefore, it appears a possible general feature of cinchona ether derivatives to possess a more populated Closed(2) conformer in polar solvents. However, when the polarity of the solvent is low, as is the case of CCl_4 and $CDCl_3$, the Open(3) conformation is the most populated for both alkaloids. Our data indicate that this could be the only conformer present in solution for PhOCD, whereas in solvents with dielectric constants comparable to that of CCl_4 (benzene and toluene) about 30 to 40% of the population of CD is represented by closed conformers.[16]

In previous studies on the application of PhOCD as chiral modifier in the platinum-catalyzed enantioselective hydrogenation of ketopantolactone (KPL), we have shown that the sense of enantiodifferentiation is reversed when PhOCD is used instead of CD in THF ($\epsilon = 7.6$) and toluene ($\epsilon = 2.3$) as the solvent,[7,8] the *S* enantiomer of pantolactone being produced in excess. Similar hydrogenation experiments performed with the chlorinated solvents $CHCl_3$ and CH_2Cl_2 used in the present study revealed a similar behavior, that is, reversing of the sense of enantiodifferentiation. Furthermore, the enantiomeric excess (*ee*) achieved under the same experimental conditions (6.8 μmol modifier, 42 mg catalyst, 5 mL solvent, 5 bar H_2, ambient temperature, 2 h) was higher in the solvent of lower polarity $CHCl_3$ (*ee* = 39%) compared to that in CH_2Cl_2 (33%). This is in line with the earlier observation that in the enantioselective hydrogenation of KPL over CD-modified platinum the *ee* decreased with increasing solvent polarity.[16] These observations suggest that the population of conformer Open(3), which decreases with solvent polarity, plays a significant role in enantiodifferentiation as advocated previously. A further interesting observation emerges from relating the results of the conformational study in $CHCl_3$ to the catalytic observation: because in this solvent the Open(3) conformer dominates for both alkaloids, the switch of enantiodifferentiation occurring upon changing from CD- to PhOCD-modified platinum cannot be traced to the different conformational behavior of these modifiers. It seems that the adsorption behavior and the sterical constraints imposed by the replacement of the OH group at C(9) by the PhO− group is the decisive factor leading to the inversion of the sense of enantiodifferentiation.

Furthermore, it remains to be clarified to which extent the interaction of the solvent molecules with the platinum surface can affect the structure of the chiral sites. This interaction is expected to be different for nonchlorinated and chlorinated solvents because the latter are able to undergo dechlorination on platinum.[35,44]

4. Conclusions

The conformational behavior of PhOCD has been studied theoretically in vacuum and experimentally using FTIR and VCD spectroscopies in selected solvents with increasing polarity and similar noncoordinating properties. Although in vacuum the behavior of PhOCD is similar to that of the parent CD, in solution and with increasing solvent polarity the Closed(2) conformer of PhOCD increases more than the same conformation of CD. Relating the conformational results to the enantiodifferentiation, these modifiers show in the platinum-catalyzed asymmetric hydrogenation of ketopantolactone that the inversion of the sense of enantiodifferentiation observed with these modifiers cannot be traced to their conformational behavior. We suggest that the sterical constraints imposed by insertion of PhO− at the C(9) position and their influence on the adsorption mode of the alkaloid are at the origin of the observed inversion of the sense of enantiodifferentiation.

Acknowledgment. We kindly acknowledge the Swiss Centre for Scientific Computing (SCSC) in Manno for computing time and the ETH Zurich and the Claude and Giuliana Foundation for financial support. Thanks are due to Mihaela Maris for carrying out the catalytic tests.

Supporting Information Available: Angles τ_1 and τ_2 of the optimized conformations of CD and PhOCD at the PM3 level of theory. This material is available free of charge via the Internet at http://pubs.acs.org.

References and Notes

(1) Kacprzak, K.; Gawronski, J. *Synthesis* **2001**, 961.
(2) Orito, Y.; Imai, S.; Niwa, S.; Nguyen, G. H. *J. Synth. Org. Chem. Jpn.* **1979**, *37*, 173.
(3) Studer, M.; Blaser, H.-U.; Exner, C. *Adv. Synth. Catal.* **2003**, *345*, 45.
(4) Bürgi, T.; Baiker, A. *Acc. Chem. Res.* **2004**, *37*, 909.
(5) Murzin, D. Y.; Mäki-Arvela, P.; Toukoniitty, E.; Salmi, T. *Catal. Rev.* **2005**, *47*, 175.
(6) Orito, Y.; Imai, S.; Niwa, S. *J. Chem. Soc. Jpn.* **1980**, 670.
(7) Diezi, S.; Szabo, A.; Mallat, T.; Baiker, A. *Tetrahedron: Asymmetry* **2003**, *14*, 2573.
(8) Diezi, S.; Mallat, T.; Szabo, A.; Baiker, A. *J. Catal.* **2004**, *228*, 162.
(9) Bonalumi, N.; Vargas, A.; Ferri, D.; Bürgi, T.; Mallat, T.; Baiker, A. *J. Am. Chem. Soc.* **2005**, *127*, 8467.
(10) Hess, R.; Krumeich, F.; Mallat, T.; Baiker, A. *J. Mol. Catal. A: Chemical* **2004**, *212*, 205.
(11) Hess, R.; Vargas, A.; Mallat, T.; Bürgi, T.; Baiker, A. *J. Catal.* **2004**, *222*, 117.
(12) Sonderegger, O.; Ho, G. M. W.; Bürgi, T.; Baiker, A. *J. Mol. Catal. A: Chem.* **2005**, *229*, 19.
(13) Baiker, A. *Catal. Today* **2005**, *100*, 159.
(14) Hiemstra, H.; Wynberg, H. *J. Am. Chem. Soc.* **1981**, *103*, 417.
(15) Aune, M.; Gogoll, A.; Matsson, O. *J. Org. Chem.* **1995**, *60*, 1356.
(16) Bürgi, T.; Baiker, A. *J. Am. Chem. Soc.* **1998**, *120*, 12920.
(17) Orglmeister, E.; Bürgi, T.; Baiker, A. *J. Catal.* **2005**, *232*, 137.
(18) Dijkstra, G. D. H.; Kellogg, R. M.; Wynberg, H. *J. Org. Chem.* **1990**, *55*, 6121.
(19) Norrby, P. O.; Kolb, H. C.; Sharpless, K. B. *J. Am. Chem. Soc.* **1994**, *116*, 8470.
(20) Dijkstra, G. D. H.; Kellogg, R. M.; Wynberg, H.; Svendsen, J. S.; Marko, I.; Sharpless, K. B. *J. Am. Chem. Soc.* **1989**, *111*, 8069.
(21) Bürgi, T.; Vargas, A.; Baiker, A. *J. Chem. Soc., Perkin Trans. 2* **2002**, 1596.

(22) Frisch, M. J.; Trucks, G. W.; Schlegel, H. B.; Scuseria, G. E.; Robb, M. A.; Cheeseman, J. R.; Zakrzewski, V. G.; Montgomery, J. A., Jr.; Stratmann, R. E.; Burant, J. C.; Dapprich, S.; Millam, J. M.; Daniels, A. D.; Kudin, K. N.; Strain, M. C.; Farkas, O.; Tomasi, J.; Barone, V.; Cossi, M.; Cammi, R.; Mennucci, B.; Pomelli, C.; Adamo, C.; Clifford, S.; Ochterski, J.; Petersson, G. A.; Ayala, P. Y.; Cui, Q.; Morokuma, K.; Malick, D. K.; Rabuck, A. D.; Raghavachari, K.; Foresman, J. B.; Cioslowski, J.; Ortiz, J. V.; Stefanov, B. B.; Liu, G.; Liashenko, A.; Piskorz, P.; Komaromi, I.; Gomperts, R.; Martin, R. L.; Fox, D. J.; Keith, T.; Al-Laham, M. A.; Peng, C. Y.; Nanayakkara, A.; Gonzalez, C.; Challacombe, M.; Gill, P. M. W.; Johnson, B. G.; Chen, W.; Wong, M. W.; Andres, J. L.; Head-Gordon, M.; Replogle, E. S.; Pople, J. A. *Gaussian 98*, revision A.11.3; Gaussian, Inc.: Pittsburgh, PA, 1998.

(23) Frisch, M. J.; Trucks, G. W.; Schlegel, H. B.; Scuseria, G. E.; Robb, M. A.; Cheeseman, J. R.; Montgomery, J. A., Jr.; Vreven, T.; Kudin, K. N.; Burant, J. C.; Millam, J. M.; Iyengar, S. S.; Tomasi, J.; Barone, V.; Mennucci, B.; Cossi, M.; Scalmani, G.; Rega, N.; Petersson, G. A.; Nakatsuji, H.; Hada, M.; Ehara, M.; Toyota, K.; Fukuda, R.; Hasegawa, J.; Ishida, M.; Nakajima, T.; Honda, Y.; Kitao, O.; Nakai, H.; Klene, M.; Li, X.; Knox, J. E.; Hratchian, H. P.; Cross, J. B.; Bakken, V.; Adamo, C.; Jaramillo, J.; Gomperts, R.; Stratmann, R. E.; Yazyev, O.; Austin, A. J.; Cammi, R.; Pomelli, C.; Ochterski, J. W.; Ayala, P. Y.; Morokuma, K.; Voth, G. A.; Salvador, P.; Dannenberg, J. J.; Zakrzewski, V. G.; Dapprich, S.; Daniels, A. D.; Strain, M. C.; Farkas, O.; Malick, D. K.; Rabuck, A. D.; Raghavachari, K.; Foresman, J. B.; Ortiz, J. V.; Cui, Q.; Baboul, A. G.; Clifford, S.; Cioslowski, J.; Stefanov, B. B.; Liu, G.; Liashenko, A.; Piskorz, P.; Komaromi, I.; Martin, R. L.; Fox, D. J.; Keith, T.; Al-Laham, M. A.; Peng, C. Y.; Nanayakkara, A.; Challacombe, M.; Gill, P. M. W.; Johnson, B.; Chen, W.; Wong, M. W.; Gonzalez, C.; Pople, J. A. *Gaussian 03*, revision C.02; Gaussian, Inc.: Wallingford, CT, 2004.

(24) Stewart, J. J. P. *J. Comput. Chem.* **1989**, *10*, 209.

(25) Becke, A. D. *J. Chem. Phys.* **1993**, *93*, 5648.

(26) Lee, C.; Yang, W.; Parr, R. G. *Phys. Rev. B* **1988**, *37*, 785.

(27) Hariharan, P. C.; Pople, J. A. *Theor. Chim. Acta* **1973**, *28*, 213.

(28) Foresman, J. B.; Keith, T. A.; Wiberg, K. B.; Snoonian, J.; Frisch, M. J. *J. Phys. Chem.* **1996**, *100*, 16098.

(29) Schaftenaar, G.; Noordik, J. H. *J. Comput.-Aided Mol. Des.* **2000**, *14*, 123.

(30) Diezi, S.; Hess, M.; Orglmeister, E.; Mallat, T.; Baiker, A. *J. Mol. Catal. A: Chem.* **2005**, *239*, 49.

(31) Berg, U.; Aune, M.; Matsson, O. *Tetrahedron Lett.* **1995**, *36*, 2137.

(32) Schürch, M.; Schwalm, O.; Mallat, T.; Weber, J.; Baiker, A. *J. Catal.* **1997**, *169*, 275.

(33) Caner, H.; Biedermann, P. U.; Agranat, I. *Chirality* **2003**, *15*, 637.

(34) Perrin, C. L.; Young, D. B. *Tetrahedron Lett.* **1995**, *36*, 7185.

(35) Ferri, D.; Bürgi, T. *J. Am. Chem. Soc.* **2001**, *123*, 12074.

(36) Chu, W.; LeBlanc, R. J.; Williams, C. T.; Kubota, J.; Zaera, F. *J. Phys. Chem. B* **2003**, *107*, 14365.

(37) Katritzky, A. R.; Jones, R. A. *J. Chem. Soc.* **1960**, 2942.

(38) Wait, S. C.; McNerney, J. C. *J. Mol. Struct.* **1970**, *34*, 56.

(39) Brüesch, P.; Günthard, H. H. *Spectrochim. Acta* **1966**, *22*, 877.

(40) Colthup, N. B.; Daly, L. H.; Wiberley, S. E. *Introduction to Infrared and Raman Spectroscopy*, 3rd ed.; Academic Press: San Diego, CA, 1990.

(41) Günzler, H.; Gremlich, H. U. *IR Spectroscopy. An Introduction*; Wiley-VCH: Weinheim, Germany, 2002.

(42) Dijkstra, G. D. H.; Kellogg, R. M.; Wynberg, H. *Recl. Trav. Chim. Pays-Bas* **1989**, *108*, 195.

(43) Reichardt, C. *Solvents and Solvent Effects in Organic Chemistry*, 3rd ed.; Wiley-VCH Verlag: Weinheim, Germany, 2003.

(44) Orglmeister, E.; Mallat, T.; Baiker, A. *J. Catal.* **2005**, *233*, 333.

(45) Furniss, B. S.; Hannaford, A. J.; Smith, P. W. G.; Tatchell, A. R. *Vogel's Textbook of Practical Organic Chemistry*, 5th ed.; Longman Scientific and Technical: Harlow, U.K., 1989.